

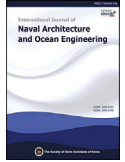


ScienceDirect

Publishing Services by Elsevier

International Journal of Naval Architecture and Ocean Engineering xx (2016) 1–12

<http://www.journals.elsevier.com/international-journal-of-naval-architecture-and-ocean-engineering/>



The effects of LNG-tank sloshing on the global motions of FLNG system

Zhi-Qiang Hu ^{a,c,*}, Shu-Ya Wang ^b, Gang Chen ^b, Shu-Hong Chai ^d, Yu-Ting Jin ^d

^a State Key Laboratory of Hydraulic Engineering Simulation and Safety, Tianjin University, Tianjin, China

^b State Key Laboratory of Ocean Engineering, Shanghai Jiao Tong University, Shanghai, China

^c School of Marine Science & Technology, Newcastle University, Newcastle upon Tyne, NE1 7RU, United Kingdom

^d University of Tasmania, Launceston, TAS, Australia

Available online ■■■

Abstract

This paper addresses a study of inner-tank sloshing effect on motion responses of a Floating Liquefied Natural Gas (FLNG) system, through experimental analysis and numerical modeling. To investigate hydrodynamic characteristics of FLNG under the conditions of with and without LNG-tank sloshing, a series of numerical simulations were carried out using potential flow solver SESAM. To validate the numerical simulations, model tests on the FLNG system was conducted in both liquid and solid ballast conditions with 75% tank filling level in height. Good correlations were observed between the measured and predicted results, proving the feasibility of the numerical modeling technique. On the verified numerical model, Response Amplitude Operators (RAOs) of the FLNG with 25% and 50% tank filling levels were calculated in six degrees of freedom. The influence of tank sloshing with varying tank filling levels on the RAOs has been presented and analyzed. The results showed that LNG-tank sloshing has a noticeable impact on the roll motion response of the FLNG and a moderate tank filling level is less helpful in reducing the roll motion response.

Copyright © 2016 Society of Naval Architects of Korea. Production and hosting by Elsevier B.V. This is an open access article under the CC BY-NC-ND license (<http://creativecommons.org/licenses/by-nc-nd/4.0/>).

Keywords: FLNG; Sloshing effect; Model test; Numerical analysis; Filling level

1. Introduction

With the increasing demands in Liquefied Natural Gas (LNG), a concept of Floating Liquefied Natural Gas (FLNG) system has been developed over the past few decades. This system with the function of mining, processing, liquefying and storing of natural gas has demonstrated great advantages over the combination of floating production platform and LNG carrier, especially for remote marine gas fields where the deployment of FLNG is a more economical alternative for pipelines tie back to shore. Although the FLNG hull is usually designed to be a typical ship type which is similar to an FPSO, it owns great volume of displacement and large LNG tanks. In addition, FLNG has higher center of gravity due to the low

density of LNG and larger waterline area. Therefore hydrodynamic characteristics of the FLNG are different from those of FPSO.

During the long-term production cycle, FLNG is located in remote locations and usually subjected to complex meta-ocean environment conditions. The loading condition of FLNG is constantly changing during the production and offloading processes. Hence, the FLNG system has to face more complicated inner LNG-tank sloshing comparing to that of a typical shuttle LNG carrier. For a partially filled LNG tank, the free surface effect causes changes of inertia and hydrostatic forces for the entire FLNG system. Unpredicted motions of the FLNG due to the free surface will, in turn, affect the sloshing in the LNG-tanks. With the effect of inner-tank sloshing, the motion response of the FLNG system, especially roll motion varies significantly with different filling levels. Nevertheless, the global hydrodynamic performance of the FLNG has direct impact on the operability of gas processing equipment on board. Severe motion may significantly reduce the entire

* Corresponding author. School of Marine Science & Technology, Newcastle University, Newcastle upon Tyne, NE1 7RU, United Kingdom

E-mail addresses: zhiqiang.hu@ncl.ac.uk, zhqhu@sjtu.edu.cn (Z.-Q. Hu).

Peer review under responsibility of Society of Naval Architects of Korea.

<http://dx.doi.org/10.1016/j.ijnaoe.2016.09.007>

2092-6782/ Copyright © 2016 Society of Naval Architects of Korea. Production and hosting by Elsevier B.V. This is an open access article under the CC BY-NC-ND license (<http://creativecommons.org/licenses/by-nc-nd/4.0/>).

Please cite this article in press as: Hu, Z.-Q., et al., The effects of LNG-tank sloshing on the global motions of FLNG system, International Journal of Naval Architecture and Ocean Engineering (2016), <http://dx.doi.org/10.1016/j.ijnaoe.2016.09.007>

production efficiency. Therefore the research on the effect of LNG tank sloshing on the global motion responses of an FLNG system is of great importance.

The coupling effect between inner tank sloshing and vessel global motion response has been studied by former researchers numerically and experimentally. Model tests investigating on the coupled tank/ship motions have been conducted over the last decade. An experiment work was conducted by Nasar et al. (2008) to study the phenomena of sloshing of liquid in partially filled tanks being mounted on a barge subjected to regular beam waves. A series of tests was also carried out in Seoul National University using an FLNG model equipped with two tanks (Nam and Kim, 2007). In this experiment, the effects of loading condition and wave amplitude in regular waves were taken into consideration. The experimental results agreed well with numerical ones calculated using impulse-response-function method (Nam et al., 2006). Zhao et al. (2014) conducted a 2D model test for an FLNG section. The model of the FLNG was allowed to move freely in roll motion mode under the excitations of an initial heel angle, band-limited waves and regular waves. Another experiment for a 3D FLNG model was also carried out by Zhao et al. (2012). It concluded that the effects of the inner-tank sloshing play an important role, particularly in the roll motion of the FLNG system.

Many studies have also been carried out on the sloshing effect of floating vessels. Kim (2002) employed a finite difference method to simulate the three-dimensional sloshing flow in anti-rolling tank while the ship motion was obtained using a time domain panel method. Kim et al. (2007) studied the coupling effects between the ship motion and sloshing flows using the impulse–response–function formulation for linear ship motion. This method showed an advantage of computational efficiency. Mitra et al. (2012) also investigated the coupling effects of ship motion with fluid oscillation inside a three-dimensional rectangular container using a time domain simulation scheme. The nonlinear sloshing was studied using a finite element model whereas nonlinear ship motion was simulated using a hybrid marine control system. For the sea-keeping problem, assumption of linear ship motion was extensively adopted and considered to be adequate in the coupling analysis (Kim et al., 2007). The sloshing flow in partially filled conditions are usually investigated by two methods: frequency domain assuming a linear sloshing flow (Molin et al., 2002; Malenica et al., 2003) and time domain adopting a nonlinear flow (Rognebakke and Faltinsen., 2003; Kim, 2001). The sloshing phenomena including wave breaking, particle splash and impact occurrence is a quite complicated problem and is beyond the scope of the study in this paper. Only the most important part of sloshing dynamics which influence the FLNG motion from a global perspective has been discussed in the study. A linear sloshing flow in frequency domain has been investigated. The well-known software package WAMIT was developed and extended by Newman (2005) to analyze the coupling problem by a linear method. In his study, wetted surface inside the tanks were included as an extension of the conventional computational domain defined by the exterior wetted surface of the body. In

the software package SESAM, similar procedures are used in the fundamental method as that in WAMIT, but the independency of the interior solutions is exploited to solve the problem separately for each tank. The numerical method considering fully dynamic fluid has been validated successfully by model test conducted by Molin (Ludvigsen et al., 2013).

To prevent violent sloshing in partially filled conditions, strict requirements for filling ratio of membrane tank have been proposed by classification societies, e.g. Register (2009) and Veritas (2006). GTT (Gaztransport&Technigaz) also introduces strict limitations in the filling levels (Delorme et al., 2005). The filling level between 10%L and 80%H is not suggested (L: length of the tank, H: height of the tank). However, sometimes FLNG has to experience the different filling levels in its tanks under severe sea conditions. Thus, the hydrodynamic performances of FLNG with different filling levels need to be comprehensively studied considering the partially filled condition is inevitable in the long-term LNG production circle. Consequently three different filling levels of 25%H, 50%H and 75%H were investigated as typical cases in this study. Ten typical GTT-shape tanks were used in both model test and numerical simulation overall.

A series of numerical simulations for the hydrodynamic performances of a conceptual FLNG system in frequency domain were carried out by using SESAM and correspondingly model tests were also conducted to verify the numerical results. The following points were focused on: 1) Hydrodynamic performances of the FLNG system with inner LNG-tank sloshing; 2) Effect of LNG-tank sloshing on the six degrees of freedoms motion responses, especially roll motion at different wave-approaching angles with different filling levels.

2. Theory of vessel motion and sloshing

Sea-keeping and inner-tank sloshing problems can be analyzed in the frequency domain using linearized potential flow theory under the assumptions of small-amplitude motions, inviscid and incompressible fluid. For the exterior flow, the Boundary Value Problem (BVP) of radiation problem is expressed as:

$$\nabla^2 \varphi_{Rj} = 0 \quad \text{In the fluid} \quad (1)$$

$$\frac{\partial \varphi_{Rj}}{\partial n} = n_j \quad \text{On the body} \quad (2)$$

$$-\nu \varphi_{Rj} + \frac{\partial \varphi_{Rj}}{\partial z} = 0 \quad \text{At still water level} \quad (3)$$

here, φ_{Rj} is the unit-amplitude radiation potentials, n indicates the unit vector normal out of the fluid domain, ν is the infinite depth wave number.

The motion equation of rigid body in six degrees of freedom can be set up in the form:

$$[M_{ij} + a_{ij}(\omega)] \ddot{\xi} + C(\omega) \dot{\xi} + K\xi = F(\omega) \quad (4)$$

here M_{ij} is the generalized mass matrix of the ship, $a_{ij}(\omega)$ is the hydrodynamic added mass matrix, $C(\omega)$ is the hydrodynamic damping matrix, ξ is the rigid body motions, K is the hydrostatic restoring matrix and $F(\omega)$ is the external force vector induced by wave.

For the inner-tank fluid, the diffraction problem doesn't exist due to the absence of incoming free wave. For the radiation problem, BVP is similar to Eqs. (1)–(3) while the free surface condition (3) should be revised because the free surface in the tank is also moving owing to the overall ship motion. In the internal fluid, radiation potential satisfies the following BVP:

$$\nabla^2 \varphi_{Rj} = 0, \quad \text{In the fluid} \quad (1)$$

$$\frac{\partial \varphi_{Rj}}{\partial n} = n_j, \quad \text{On the body} \quad (2)$$

$$-\nu \varphi_{Rj} + \frac{\partial \varphi_{Rj}}{\partial z} = \dot{Z}_0, \quad \text{At still water level} \quad (5)$$

In Eq. (5), \dot{Z}_0 comes from the velocity of overall ship motion and its value for vertical motion modes (heave, roll and pitch) is not equal to zero which leads to the non-homogeneity of Eq. (5). For the horizontal motions, $\dot{Z}_0 = 0$ and the BVP for internal and out fluid domain keeps the same.

In the process of solving BVP for internal fluid, Eq. (5) is replaced by Eq. (3) so that the BVP solver for the outer fluid domain can be re-used for the inner tank. The added mass of the inner-tank fluid in the vertical mode obtained by this method will not be correct because the particular solution φ^p generated by non-homogeneity of Eq. (5) is ignored.

$$\text{In the vertical modes, } \varphi^p = -\frac{\dot{Z}_0}{\nu} \quad (6)$$

$$\text{So that } \frac{\partial \varphi^p}{\partial t} = -\frac{ig}{\omega} \dot{Z}_0 = gZ_0 \quad (7)$$

The restoring pressure contribution is also modified by the vertical velocity of the mean free surface and the total pressure is calculated from the linearized Bernoulli's equation:

$$p = -\rho \frac{\partial}{\partial t} (\varphi + \varphi^p) - \rho g [z - Z_0] = -\rho \frac{\partial \varphi}{\partial t} - \rho g z \quad (8)$$

It is proved by Eq. (8) that in the equations of motion the contribution from the vertical velocity is canceled by the hydrostatic restoring pressure (Ludvigsen et al., 2013). Thus the added mass can be calculated based on the velocity potential obtained from Eqs. (1)–(3), as long as the global restoring is also calculated using the same approach. Furthermore, it is proved by Malenica et al. (2003) that the free surface condition Eq. (5) for roll and pitch keeps the same with the external fluid field by taking the mean position of the internal free surface as the local reference point. In this way, the inner-tank sloshing problem can be totally solved as the traditional sea-keeping radiation problem.

Under this circumstance, the equation of the rigid body motions in six degrees of freedom can be set up as follows:

$$\begin{aligned} & [M_{ij} + a_{ij}(\omega) + a_{ij-tank}(\omega)] \ddot{\xi} + [C(\omega) + C_{44}^*(\omega)] \dot{\xi} \\ & + [K_{ij} + K_{ij-tank}] \xi = F(\omega) \end{aligned} \quad (9)$$

here, $K_{ij-tank}$ is the hydrostatic restoring matrix for tanks and it is usually negative so the global restoring force of the coupled system will be reduced. It should be noticed that the mass of the liquid should not be included in the total mass M_{ij} because the inner-tank dynamic inertia is totally described by the added mass $a_{ij-tank}(\omega)$. Viscous effect for roll is replaced by adding the liner equivalent damping coefficient $C_{44}^*(\omega)$ into the damping matrix $C(\omega)$.

Based on the theories mentioned above, numerical analysis on the hydrodynamics of the FLNG vessel ballasted in liquid cases with three different filling levels can be carried out. For an FLNG with the equivalent filling levels in solid-ballast conditions, the existing diffraction-radiation method is adopted. RAOs of the six-degree of freedom motions are given in the following section. The detailed mathematical background information can be found in Ludvigsen et al. (2013).

3. Description of the FLNG system

3.1. FLNG system

In the present study, a conceptual single point moored FLNG system has been selected as the reference vessel. The main particulars of the FLNG are presented in Table 1. The FLNG vessel has a total length of 340 m, a breadth of 61 m and a depth of 37 m. It is designed to be located in the site with water depth of 1500 m in South China Sea and it is moored by 15 mooring lines attached to an internal turret. Ten identical double-row arranged LNG tanks are placed inside of the FLNG as shown in Fig. 1. In this numerical study, the hydrodynamic performances of the FLNG vessel with three filling levels of 25%H, 50%H, and 75%H were investigated. Experiment was only carried out with one filling level of 75% H in a scale of 1:60.

Table 1
Principal particulars of the FLNG vessel in liquid ballast conditions.

Designation	Signal	Unit	LC1 (25%)	LC2 (50%)	LC3 (75%)
Length between perpendiculars	Lpp	m	330	330	330
Breadth	B	m	61	61	61
Depth	D	m	37	37	37
Draft	T	m	15.4	15.6	16.8
Displacement	Δ	ton	274,700	278,804	302,237
Center of gravity above base	KG	m	22.4	22.3	22.6
Center of gravity from AP	LCG	m	164.3	162.5	162
Radius of roll gyration	RXX	m	25.3	23.8	23.5
Radius of pitch gyration	RYY	m	84.6	85.8	85.2
Radius of yaw gyration	RZZ	m	85.6	86.7	86

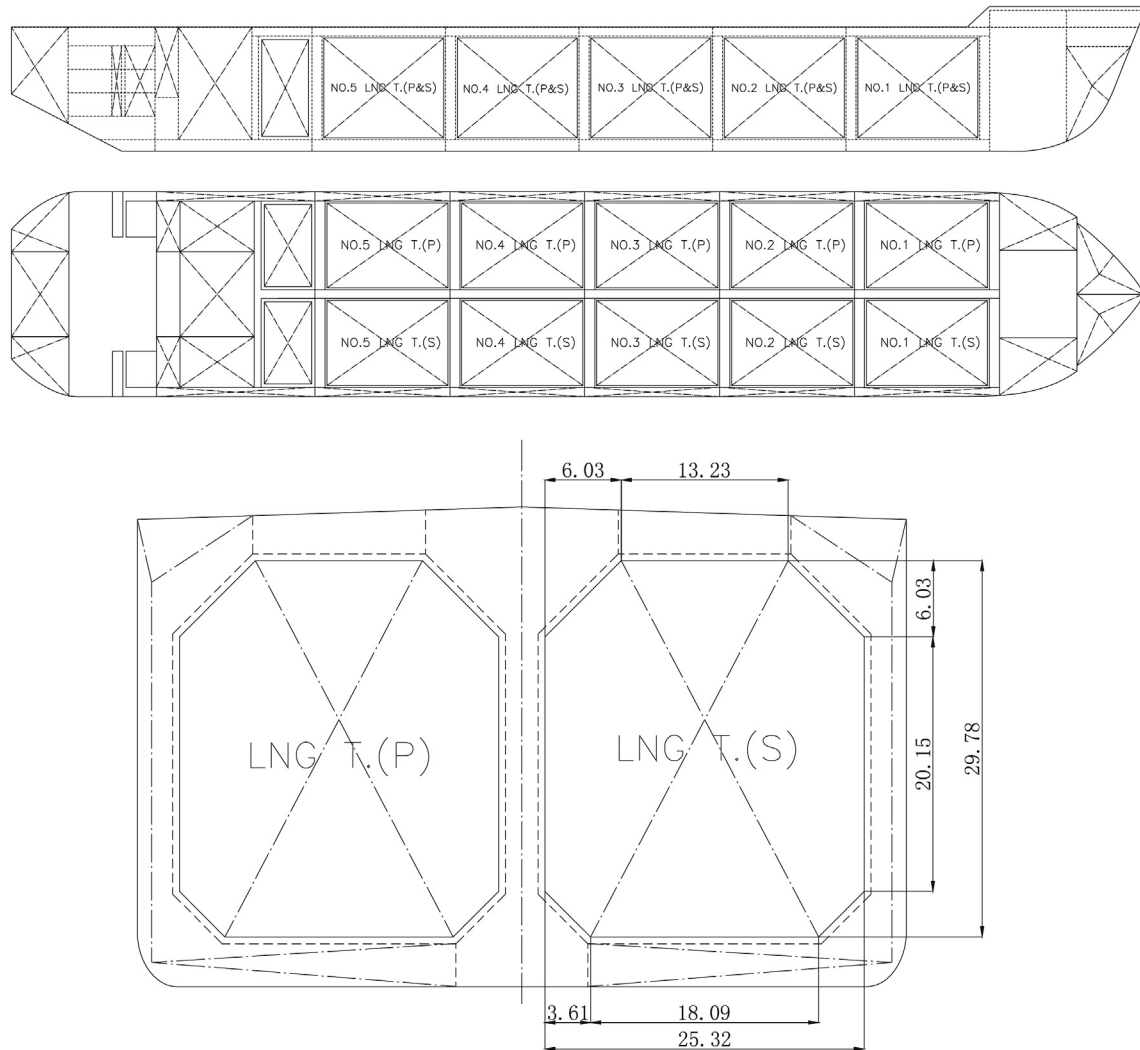


Fig. 1. Location of the LNGC tanks in FLNG system: side view, top view and cross-section view.

3.2. LNG tank

The LNG tanks are arranged in two paralleled rows with a separation distance of 11 m between the central line of each tanks and the center plane ($y = 0$) of the vessel in transverse. The dimensions of the LNG tanks are listed in Table 2. The locations of the LNG tanks inside of FLNG are also given in Fig. 1.

4. Hydrodynamic modeling

Numerical analysis in frequency domain based on the potential theory were conducted to determine RAOs of the FLNG

vessel, and to be verified by the experiment results. To simulate a vessel with LNG tanks, a panel model including tanks was firstly established as shown in Fig. 2. For a full dynamic approach newly implemented in SESAM, the panel model consists of the vessel hull on which the external wave loads are applied, and the compartments in which the sloshing effect is applied. The mass model is divided into two parts: the hull mass and the compartment mass. The former one is defined by the hull mass properties including center of gravity and radii of gyration and the latter one is calculated automatically according to the loading capacity and liquid density. The hull mass characteristics used in simulation are as shown in Table 3.

For a vessel in solid ballast conditions, the inner tanks were not required anymore. Mass model which represents the mass distribution was defined by the center of gravity and radii of gyration presented in Table 3. It is noted that in all loading conditions the mass properties of the whole vessel in solid and liquid ballast conditions were kept consistent in the simulation.

The motion responses RAOs were calculated for various wave heading angles with 15° interval and the intermediated values for other angles are interpolated. The numerical

Table 2
Dimension of the LNG tanks in both full scale and model scale.

	Unit	Full scale	Model scale
Length	m	37	0.617
Breadth	m	25.32	0.42
Height	m	29.78	0.496

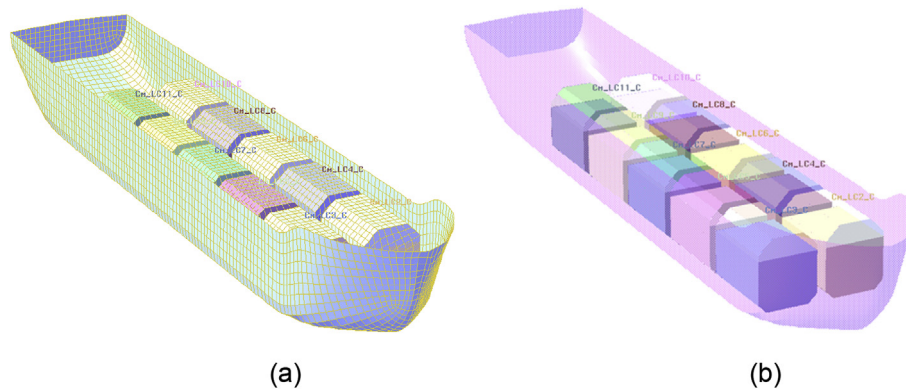


Fig. 2. (a) Panel model of liquid-ballast FLNG. (b) Structure model of liquid-ballast FLNG.

Table 3

Characteristics of the FLNG vessel without considering the inner tank.

Designation	Signal	Unit	LC1 (25%)	LC2 (50%)	LC3 (75%)
Displacement	Δ	ton	213005.9	155415.9	117155.6
Center of gravity above base	KG	m	26.3	30.6	34.3
Center of gravity from AP	LCG	m	156.4	139.4	115.4
Radius of roll gyration	RXX	m	25	24.6	15.4
Radius of pitch gyration	RYY	m	88.8	96	69.1
Radius of yaw gyration	RZZ	m	90.5	97.8	72.3

simulation results were also compared with the experimental results, showing fair agreement.

5. Experimental set-up

Model tests were conducted in Deep-water Offshore Basin at Shanghai Jiao Tong University. The main dimensions of the basin are 50 m × 40 m × 10 m. A horizontal mooring system with four soft lines was introduced to constraint the horizontal drift motion of FLNG model. The soft mooring line system was made of springs and chains to achieve a desired horizontal stiffness, which have limited influences on the motions induced by 1st-order wave force. The angle between the longitudinal central line of the vessel and each mooring line was 45° and the separation angle of the neighboring lines was 90°.

Motion response model tests of the FLNG vessel, under two wave heading conditions of 180° and 150° and in two ballast conditions both in solid and liquid filling cases, were carried out in the basin. The configuration of the model tests in the basin, along with the layout can be seen in Fig. 3(a) and (b). More details can be found in the reference from Xie et al. (2015). To investigate the effect of inner tank sloshing on vessel motions, the characteristics of the FLNG vessel including displacement, center of gravity and radii of gyration in solid and liquid ballasting condition should keep identical. The motion responses of the vessel in six degrees of freedom have been captured by sampling frequency of 20 Hz. LNG tanks used in model test are as shown in Fig. 4. All of the RAOs obtained from experiment were used for the validation of numerical analysis results.

In this study, decay test of FLNG model in both solid and liquid ballast conditions in still water were also carried out. In

the test, an initial disturbance was given to initiate the vessel motion for a free decay. Non-dimensional damping coefficients and natural periods of FLNG motion were measured in 25%H, 50%H and 75%H filling condition in both liquid and solid case for the calculation of viscous damping. An example results are given in Fig. 5.

Both white noise test and decay test of FLNG model were carried out before the testing program. In the white noise irregular wave tests, wave heights were varied 0–3.24 m and periods from 5 s to 25 s in full scale. Power spectrum density of white noise is shown in Fig. 6.

6. Results and discussions

6.1. Damping correction

The hydrodynamic performance of the FLNG with 75%H inner tanks filling level was firstly obtained through numerical analysis. The corresponding model test in both solid and liquid ballast conditions were carried out to verify the numerical model. Based on the validated numerical model, hydrodynamics of the FLNG system with inner tanks sloshing at low filling levels were investigated.

In 25%H, 50%H and 75%H tank filling conditions, viscous damping coefficients for the numerical model were determined from decay tests. The calculation method is as follows:

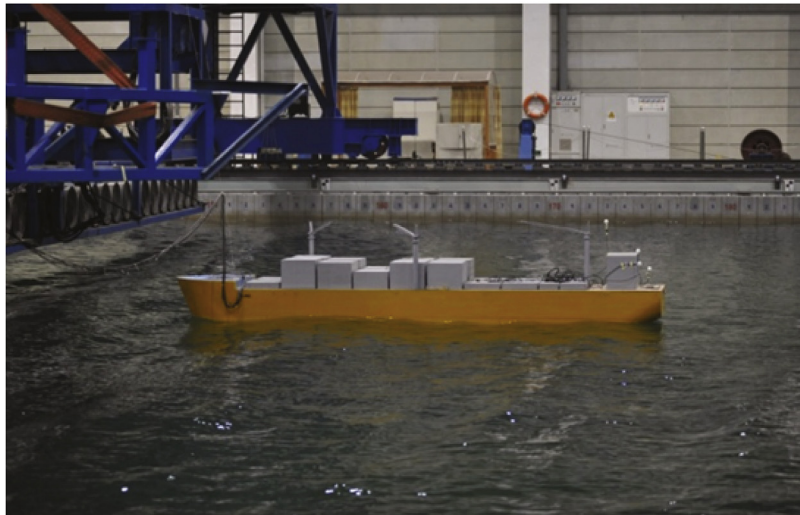
$$C_{44}^* = 2N - \lambda_{44} = 2\nu I'_{xx} - \lambda_{44} = 2\mu\omega_n I'_{xx} - \lambda_{44} \quad (10)$$

where N is roll-damping moment coefficient and λ_{44} is damping coefficient in natural period; ν and I'_{xx} indicate roll-damping coefficient and roll moment of inertia; μ and ω_n obtained from the decay tests stand for dimensionless damping coefficient and natural frequency of roll motion.

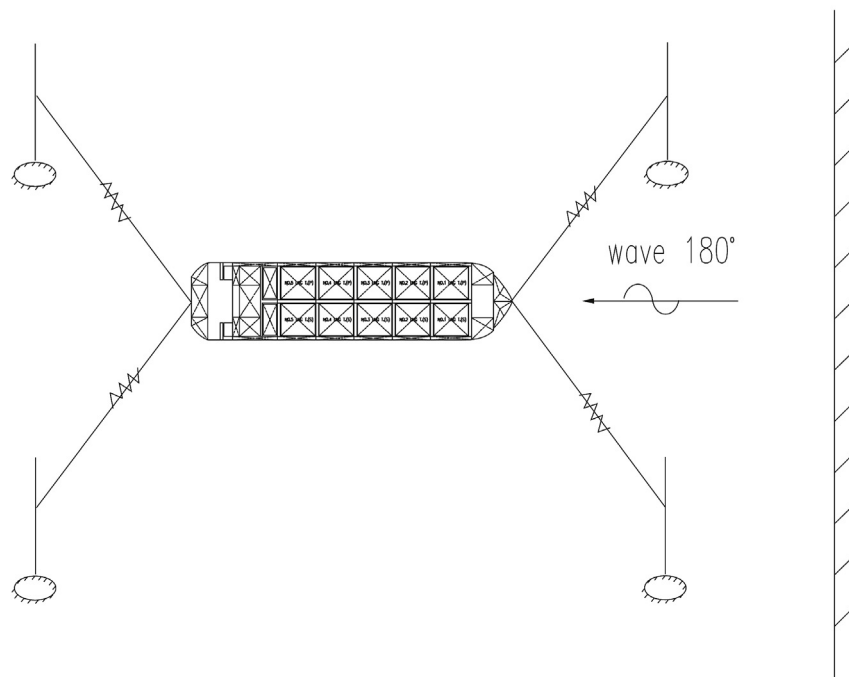
In the software SESAM, viscous effect can be included by adding liner equivalent damping coefficient. In this study, the liner equivalent damping coefficient C_{44}^* achieved above is added to $C_{44}(\omega)$ (Lee, 2008)

$$C_{44}^*(\omega) = 2\gamma\sqrt{\{M_{44} + a_{44}\}K_{44}} \quad (11)$$

where, γ is the damping ratio defined as system damping over critical damping.



(a)



(b)

Fig. 3. (a) FLNG vessel model test setup in the basin. (b) Configuration of the horizontal mooring system.

In the numerical analysis, 9.1% and 3.8% of extra critical damping were added into the system for the 75%H condition; For the 50%H condition, 11.3% and 5.6% of extra critical damping were added; And for the 25%H case, 10.3% and 4.6% of the critical damping were added.

6.2. Natural period determination

Before analyzing the results, the natural periods of LNG tank was calculated and revised by a correction factor for its prismatic shape with chamfered bottom. Formula (12) and (13)

are derived by Faltinsen and Timokha (2009) and the natural frequencies of LNG tank are as shown in Table 4.

$$\omega_{r,j} = \sqrt{\frac{i\pi g \tanh\left(\frac{i\pi h}{l}\right)}{l}}, \quad i = 1, 2, 3 \quad (12)$$

where $\omega_{r,j}$ is the natural sloshing frequencies of the i th mode for a rectangular tank, h indicates the filling height inside the tank and l denotes the length of free surface in the direction of

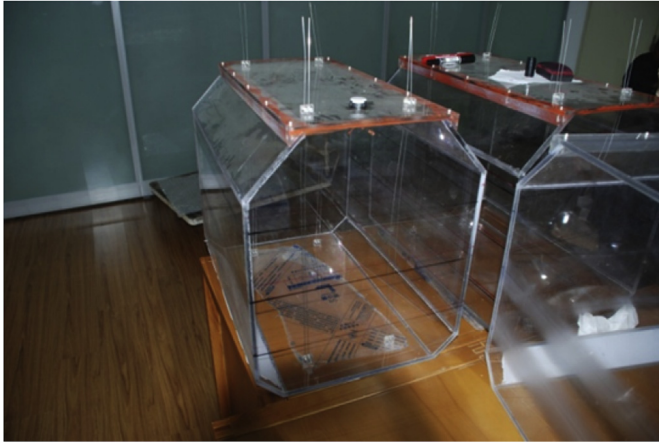


Fig. 4. LNG tanks setup in model test.

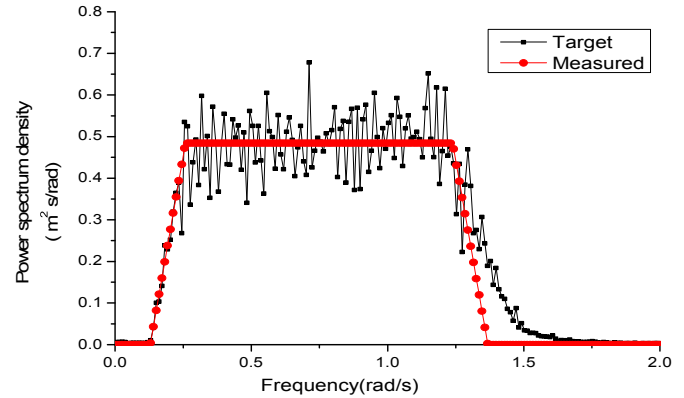


Fig. 6. Power spectrum density of the white noise.

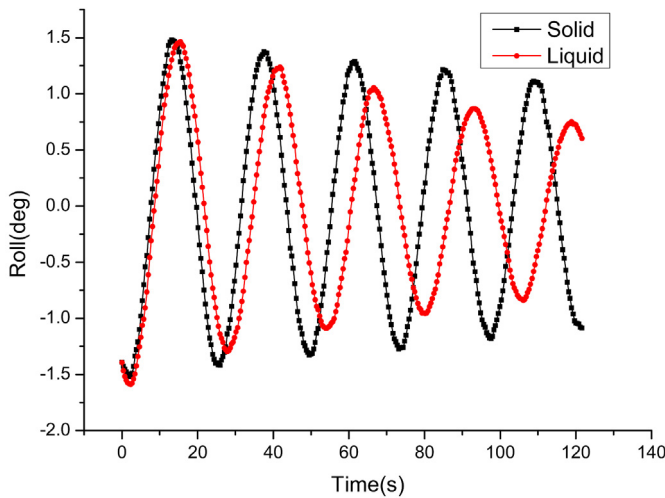


Fig. 5. Roll decay curve with 75%H filling level in solid and liquid conditions.

tank movement (for a transverse sloshing case, l means the breadth of tank).

For prismatic tanks with chamfered bottom, a correction factor should be proposed:

$$\frac{\omega_{r,j}^2}{\omega_{r,j}^2} = 1 - \frac{\delta_1 \delta_2^{-1} \sinh^2\left(\frac{\pi i \delta_2}{l}\right) - \delta_1 \delta_2^{-1} \sin^2\left(\frac{\pi i \delta_2}{l}\right)}{\pi i \sinh\left(\frac{2\pi i h}{l}\right)} \quad (13)$$

where $\omega'_{r,j}$ is the corrected natural frequency of the i th mode for prismatic tanks. δ_1 and δ_2 are horizontal and vertical dimensions of the chamfer respectively.

The RAOs of the FLNG vessel with 75%H LNG-tank filling levels are plotted in Fig. 7(a)–(f). For sway, roll and yaw, a wave heading angle of 150° was chosen in order to demonstrate more obvious vessel motion responses.

One can observe from Fig. 7(a) and (b) that the surge and sway motion of the vessel are more pronounced in long-period waves which indicates that low frequency motions will be of primary concerns for these two response modes. For heave

Table 4

Natural periods of tank sloshing in first-order motion.

Filling case	Transverse(s)	Longitudinal(s)
25%H	6.67	9.18
50%H	6.35	8.66
75%H	5.81	7.31

motion, the resonant response is at about 11.6 s and the RAO value approaches 1.0 as the wave period increases. As shown in Fig. 7(d), the roll motion response from numerical analysis agrees well with the experimental data in the wave heading of 150° . The results also demonstrate that the resonance of roll motion exists in large period waves, which differs from that of a FPSO hull. This could be caused by a higher center of gravity, greater volume of liquid inside of the LNG-tanks and larger waterline area of FLNG hull.

As presented in Fig. 8(a) and (b), peak value of roll motion RAO is sensitive to the variation of wave approaching angles over the entire wave period range for 25%H and 50%H filling conditions. This is mainly due to the huge wave loads acting on a vessel with a high center of gravity and large waterline area. Thus, the turret-mooring system is extremely important for the safe operation of the FLNG system as it allows the vessel to weathervane along the wave-approaching angle, which avoids unexpected large roll motions for this type of floating structures. The pitch and yaw RAO curves demonstrate a resonant response happening at around 16.5 s. It should be noticed that the yaw motion response obtained from the numerical analysis doesn't match well with the experimental data at the wave heading of 150° . A variation of 82.7% in peak response amplitude was observed. This inconformity could be caused by the horizontal mooring system used in the white noise test where the system undermined the response of yaw motion in some extent.

Overall, the fair correlation between numerical and experimental results demonstrates that the presented dynamic method is feasible to predict global motion responses of floating structures coupled with inner tank sloshing. Applying this technique, the effect of LNG-tank sloshing on the hydrodynamic performance of the FLNG vessel can be properly addressed.

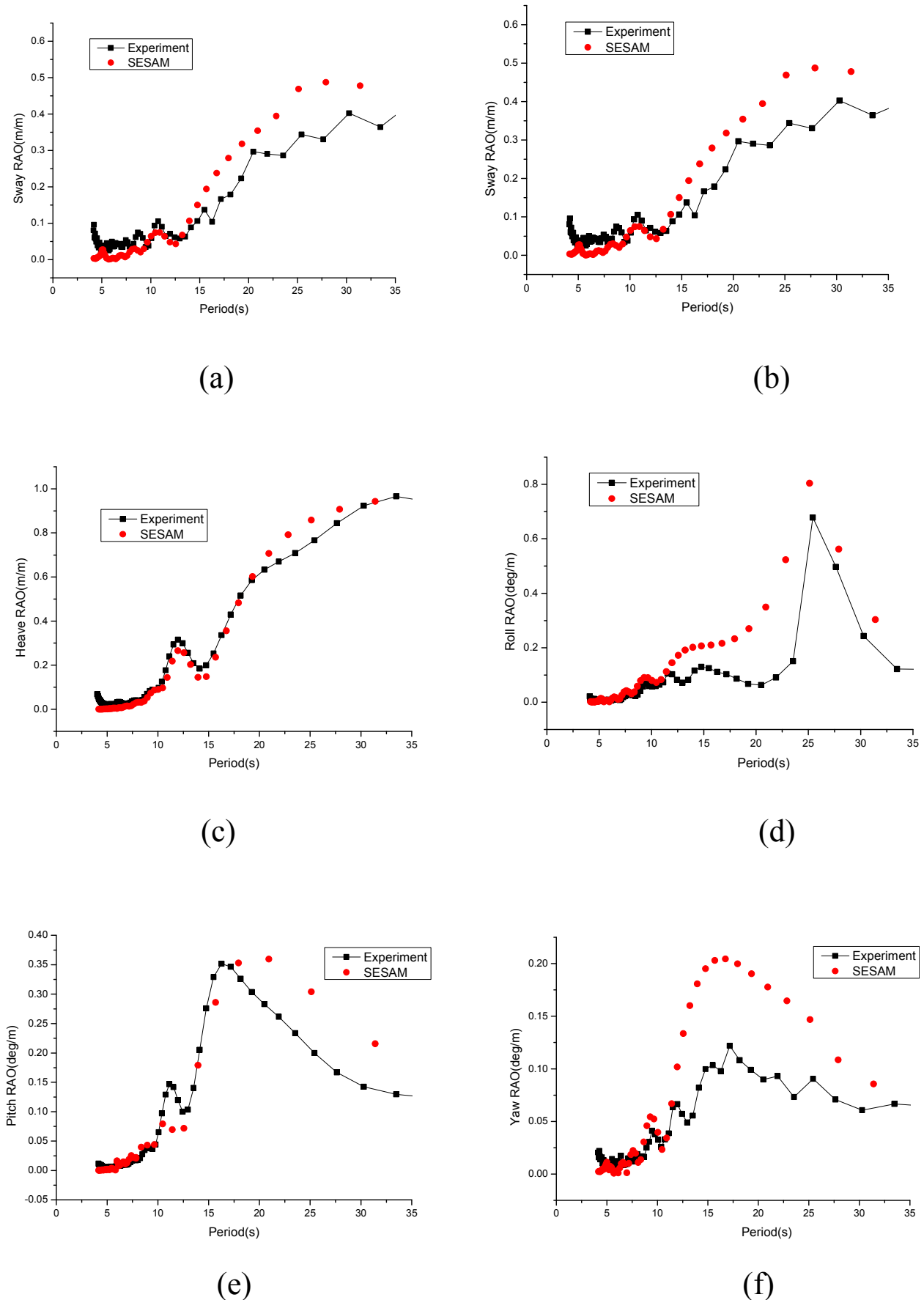


Fig. 7. Numerical and Experimental RAOs of FLNG for the 75%H liquid-ballast case (surge, pith and heave: in the heading sea of 180°; sway, roll and yaw: in the wave heading of 150°).

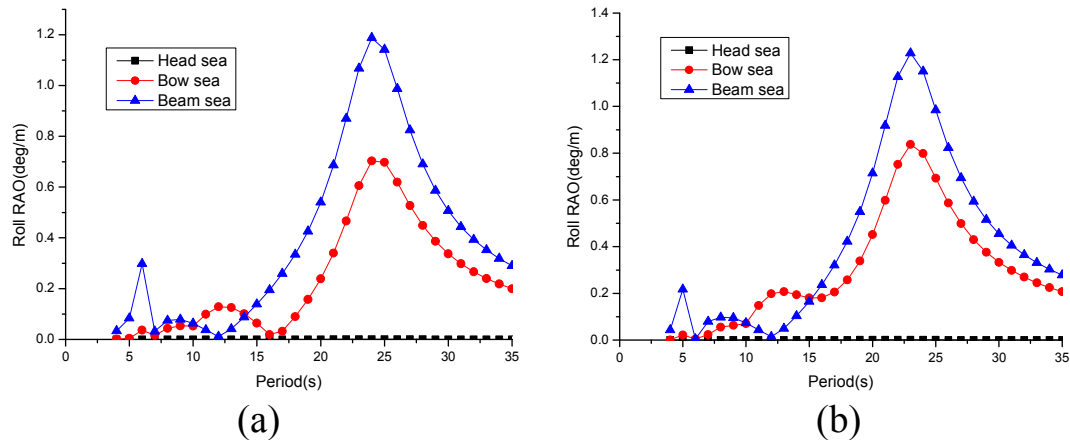


Fig. 8. Numerical RAOs of the liquid-ballast FLNG for roll motion in three wave headings (bow sea: 135°): (a) 25%H filling level (b) 50%H filling level.

6.3. Effect of sloshing in tank

As shown from Fig. 9(a)–(f), the computed motion responses of a solid-ballast FLNG vessel agrees well with the experimental data in all six modes of motion. Therefore, the numerical model of solid-ballast has been verified and can be applied to predict the hydrodynamic performance of the FLNG in any solid filling conditions.

It can be observed that the LNG-tank sloshing plays an important role in roll motion while its influence on the other motion modes is relatively small or negligible. Characteristic values including resonant period and its corresponding motion response for 25%H and 50%H filling conditions in the wave heading of 150° are illustrated in Tables 5 and 6 respectively. It was found that the discrepancies in the resonant period and amplitude between the solid and liquid ballast conditions are small in all of the motion modes except roll.

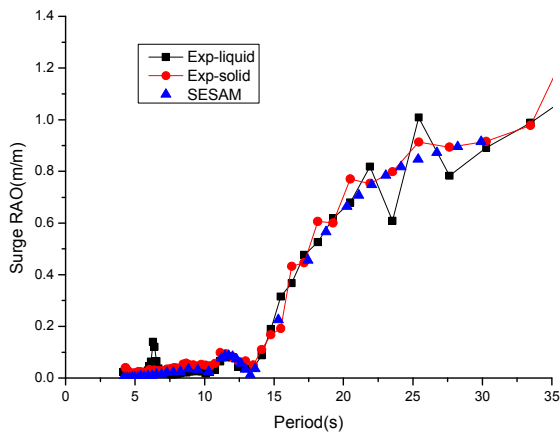
Figs. 9(a) and 10(a) show the resonance in surge response of the FLNG appears peaks at around 6.28 s and 8.60 s which is also the first-order resonant period of the LNG-tank with two different filling levels, 75%H and 25%H respectively. The sway motion, as presented in Figs. 9(b) and 10(b), shows similar phenomena. This feature, which was also found by Newman (2005), indicates evident influence of LNG-tank sloshing on the global motions of floating structures at high frequency waves. It also can be seen that the sloshing hardly affects the heave motion. This phenomenon coincides with the conclusions summarized by Malenica et al. (2003) that the heave motion of inner tank liquid will not generate free surface deformations, the corresponding added mass in heave is equal to the mass of liquid inside the tank. One can also find in Fig. 9(e) that the RAO of pitch motion presents good agreement between the solid and liquid ballast conditions, with a peak RAO value reaching 0.33°/m at a resonant period of 15.32 s in heading sea condition. This may be due to the reason that the hydrostatic restoring force stiffness of tanks in longitudinal direction is far less than the FLNG pitch radius of gyration, thus the sloshing effect on the pitch motion is negligible. From Fig. 9(f), one can also draw the conclusion that sloshing does not have a significant effect on yaw motion.

6.4. Effect of sloshing on roll motion

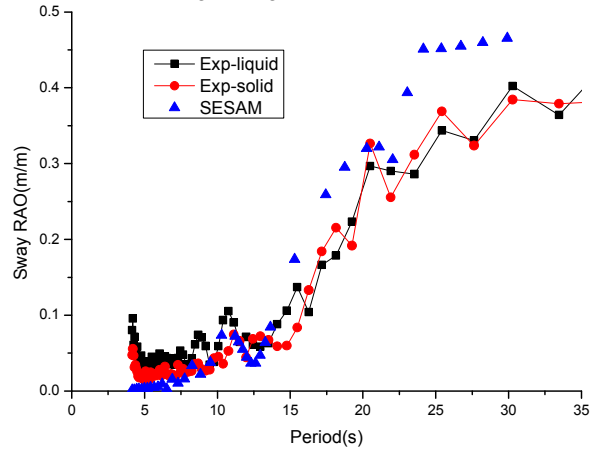
Inner tank sloshing has a significant influence on roll motion of the FLNG vessel. As shown in Fig. 9, with the effect of tank sloshing, the response amplitude of roll motion shifts apparently from that captured at the solid ballast condition with a decrease of 52.4%. It can be concluded from Fig. 12 that in quartering and beam sea conditions, the reduction of roll RAO amplitude at liquid ballast conditions are 47% and 63% respectively. The effect of sloshing reaches a minimum in quartering sea condition. This may be caused by the distinction of phase difference between sloshing induced force and wave force (Zhao et al., 2013a,b). In all of the three filling conditions, the sloshing effect on the FLNG system is profound and the sloshing induced force and wave force is more likely to be in the opposite direction and located on the same magnitude. In quartering sea, their phase difference obtains a minimum. The inconsistent conclusions has been drawn in 50%H filling condition in which the decrease shows a positive correlation with the wave-approach angle and so does in 25% H case. This phenomenon indicates the uncertainty of the sloshing effect on the FLNG system which needs further study due to the continuous change in wave heading during FLNG production circle.

The comparison of roll motion response between solid and liquid ballast conditions at different filling conditions has been illustrated in Fig. 12. One can find for all three filling conditions, the effect of LNG-tank sloshing on the roll motion is positive for the studied wave-approaching angles, which means the anti-rolling effect of tank sloshing can be taken into consideration when the FLNG system is properly designed.

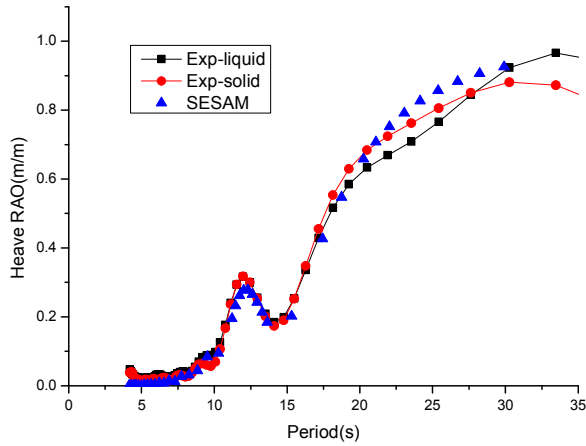
It can also be observed from Fig. 12 that in quartering sea, the reduction of motion amplitudes caused by sloshing effect are 56%, 39% and 47% (in ascending filling level order) and the series in beam sea condition are 58%, 51% and 63%. It is interesting that a moderate filling level is less helpful in reducing roll response. In the numerical method adopted in the study, the LNG-tank sloshing effect is considered mainly by importing the added mass and restoring force of sloshing fluid. The added mass matters more in a high filling level due to a



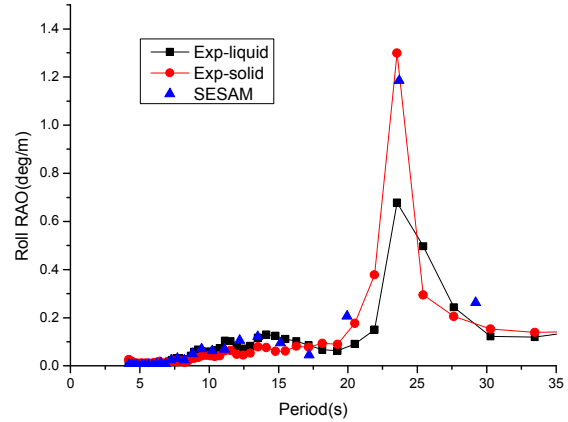
(a)



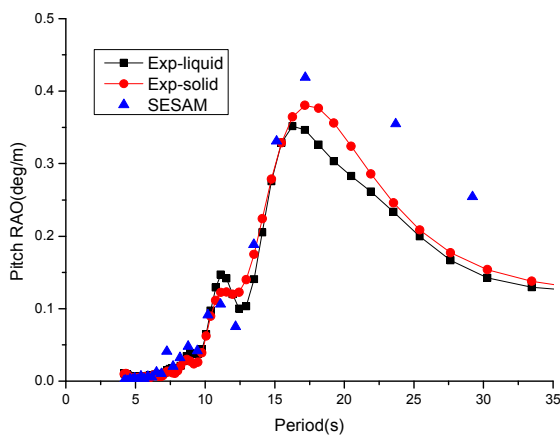
(b)



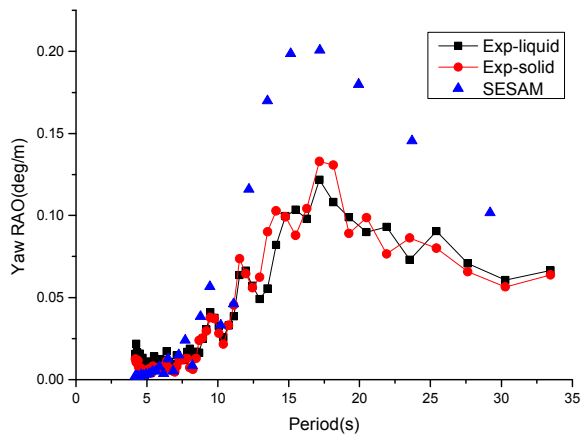
(c)



(d)



(e)



(f)

Fig. 9. Numerical and Experimental RAOs of the FLNG with and without considering the inner-tank sloshing for the 75%H filling level (surge, pitch and heave: in wave heading of 180°; sway, roll and yaw: in the wave heading of 150°).

Table 5
Characteristic values for 25% filling condition in the wave heading of 150°.

Motion mode	Item	Unit	Liquid	Solid
Heave	R.P	s	11.42	11.42
	C.M.R	m/m	2.46E-01	2.53E-01
Roll	R.P	s	25.12	22.84
	C.M.R	deg/m	4.52E-01	1.01E+00
Pitch	R.P	s	17.94	17.44
	C.M.R	deg/m	4.16E-01	4.17E-01

Table 6
Characteristic values for 50% filling condition in the wave heading of 150°.

Motion mode	Item	Unit	Liquid	Solid
Heave	R.P	s	11.42	11.42
	C.M.R	m/m	0.247	0.252
Roll	R.P	s	22.84	20.93
	C.M.R	m	0.588	0.845
Pitch	R.P	s	17.94	17.44
	C.M.R	deg/m	0.421	0.435

larger inertia. One can see from Fig. 11 that the change of added mass of the whole vessel under the effect of inner tank sloshing. In high wave period range, where the negative added mass balances a portion of the body mass resulting the mass term turns to be negative, the RAO can be much smaller than that in solid ballast cases where the maximum of added mass rises in the resonant frequency of roll motion. In a word, with the change of filling levels, the mass term varies under the influence of both body mass and inertia of inner-tank fluid and this may be the reason why a 50%H fill ratio shows an insignificant influence.

Another phenomenon that can be seen in Fig. 12 is the similarity of response amplitudes in three cases in beam sea condition. The results show the insensitivity of FLNG to LNG-tank filling levels in a large wave-approaching angle.

7. Conclusions

In this paper, the coupling effect between global FLNG motions and inner tank sloshing are studied experimentally

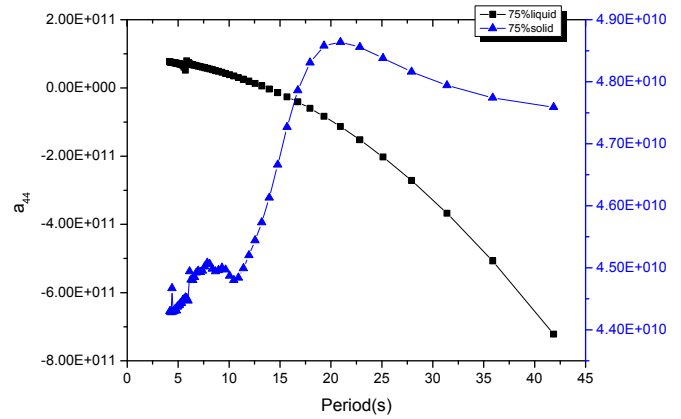


Fig. 11. Added-mass for both liquid and solid cases with 75%H filling level.

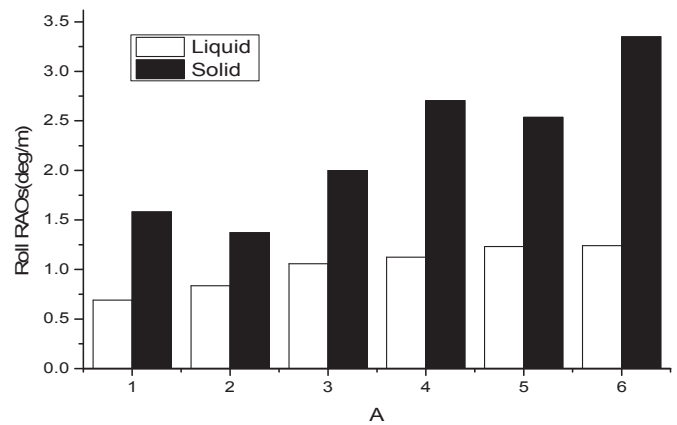


Fig. 12. Comparison of response amplitudes of roll motion (1, 2, 3: in quartering sea with filling levels of 25%H, 50%H, 75%H; 4, 5, 6: in beam sea with filling levels of 25%H, 50%H, 75%H).

and numerically. Based on the present computational results and experimental observations, following conclusions have been drawn:

- 1) The fair agreement of numerical and experimental results shows that the full dynamic method for inner LNG-tank

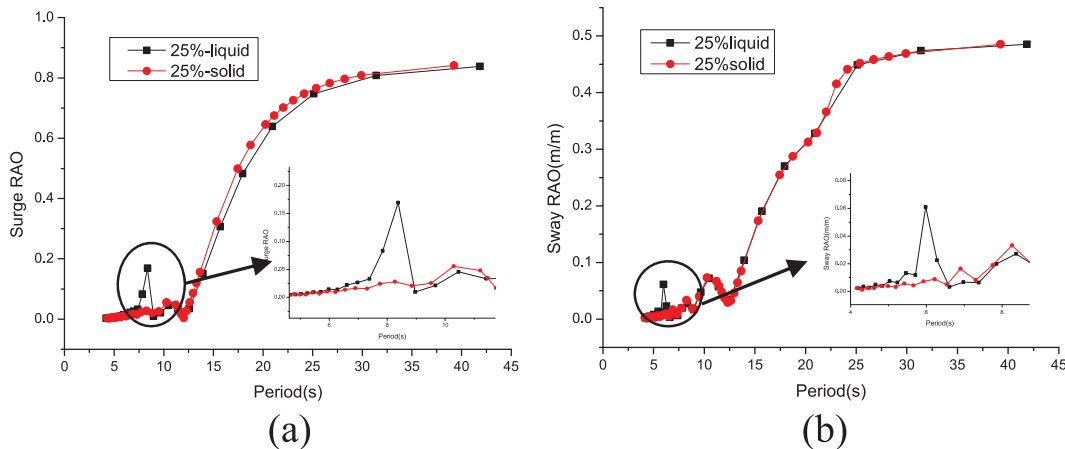


Fig. 10. Numerical RAOs of the FLNG with and without considering the inner-tank sloshing for the 25%H filling condition: (a) surge (b) sway.

sloshing can be confidently used in the motion response prediction for an FLNG.

- 2) The effect of inner tank sloshing on the global motion response in the modes of pitch, heave and yaw are negligible. For surge and sway motion, a noticeable peak response appears near the first-order resonant period of the LNG-tank.
- 3) The impact of inner tank sloshing on roll motion has been demonstrated to be related with the wave-approaching angle and inner-tank filling level. The effect of sloshing reaches its minimum in quartering sea at the high tank filling level (75%H). At the low LNG filling level (25%H), sloshing shows a positive correlation with the wave-approaching angle. For the moderate tank filling condition (50%), the sloshing is less helpful in reducing roll response. In beam sea condition, the roll response demonstrates lack of sensitivity to filling level.

Acknowledgement

This work was supported financially by State Key Laboratory of Hydraulic Engineering Simulation and Safety, Tianjin University (HESS-1404). This source of support is acknowledged gratefully by the authors.

References

- Delorme, L., Iglesias, A.S., Perez, S.A., 2005. Sloshing loads simulation in LNG tankers with SPH. In: International Conference on Computational Methods in Marine Engineering, Barcelona.
- Faltinsen, O.M., Timokha, A.N., 2009. Sloshing. Cambridge University Press, New York.
- Kim, Y., 2001. Coupled analysis of ship motions and sloshing flows. In: 16th International Workshop on Water Waves and Floating Bodies, Hiroshima.
- Kim, Y., 2002. A numerical study on sloshing flows coupled with ship motion—the anti-rolling tank problem. *J. Ship Res.* 46, 52–62.
- Kim, Y., Nam, B., Kim, D., Kim, Y., 2007. Study on coupling effects of ship motion and sloshing. *Ocean Eng.* 34, 2176–2187.
- Lee, S.J., 2008. The Effects of LNG-sloshing on the Global Responses of LNG-carriers. Texas A&M University.
- Ludvigsen, A., PAN, Z.Y., Gou, P., Vada, T., 2013. Adapting a linear potential theory solver for the outer hull to account for fluid dynamics in tanks. In: Proceeding of the 32th OMAE 2013, Nantes, France.
- Malenica, S., Zalar, M., Chen, X., 2003. Dynamic coupling of seakeeping and sloshing. In: 13th International Offshore and Polar Engineering Conference, ISOPE, Honolulu, HI, pp. 25–30.
- Mitra, S., Wang, C., Reddy, J., Khoo, B., 2012. A 3D fully coupled analysis of nonlinear sloshing and ship motion. *Ocean Eng.* 39, 1–13.
- Molin, B., Remy, F., Rigaud, S., Jouette de, C., 2002. LNG FPSOs: frequency domain, coupled analysis of support and liquid cargo motion. In: Proceedings of the 10th International Maritime Association of the Mediterranean (IMAM) Conference, Rethymnon, Greece.
- Nam, B., Kim, Y., Kim, D., 2006. Nonlinear effects of sloshing flows on ship motion. In: International Workshop on Water Waves and Floating Bodies, Loughborough, UK.
- Nam, B.-W., Kim, Y., 2007. Effects of sloshing on the motion response of LNG-FPSO in waves. In: The 22nd Workshop on Water Waves and Floating Bodies, Plitvice, Croatia.
- Nasar, T., Sannasiraj, S., Sundar, V., 2008. Experimental study of liquid sloshing dynamics in a barge carrying tank. *Fluid Dyn. Res.* 40, 427–458.
- Newman, J., 2005. Wave effects on vessels with internal tanks. In: Proceedings of the 20th Workshop on Water Waves and Floating Bodies, Spitsbergen, Norway.
- Register, Lloyd, 2009. Sloshing Assessment Guidance Document for Membrane Tank LNG Operations. LR Guidance Notes.
- Rognebakke, O.F., Faltinsen, O.M., 2003. Coupling of sloshing and ship motions. *J. Ship Res.* 47, 208–221.
- Veritas, Det Norske, 2006. Sloshing Analysis of LNG Membrane Tanks. DNV Classification Notes.
- Xie, Z.T., Yang, J.M., Hu, Z.Q., Zhao, W.H., Zhao, J.R., 2015. The horizontal stability of an FLNG with different turret locations. *Int. J. Nav. Archit. Ocean Eng.* 7, 244–258.
- Zhao, W.H., Yang, J.M., Hu, Z.Q., 2013a. Effects of sloshing on the global motion responses of FLNG. *Ships Offshore Struct.* 8, 111–122.
- Zhao, W., Yang, J., Hu, Z.Q., Tao, L.B., 2014. Coupled analysis of nonlinear sloshing and ship motions. *Appl. Ocean Res.* 47, 85–97.
- Zhao, W.H., Yang, J.M., Hu, Z.Q., Xiao, L.F., Peng, T., 2013b. Experimental and numerical investigation of the roll motion behavior of a floating liquefied natural gas system. *Sci. China* 56 (3), 629–644.
- Zhao, W.H., Yang, J.M., Hu, Z.Q., Xiao, L.F., 2012. Experimental investigation of effects of inner-tank sloshing on hydrodynamics of an FLNG system. *J. Hydrodyn. Ser. B* 24, 107–115.